

Communication

**A Highly Fluorescent Nucleobase Molecular Rotor**

Ashkan Karimi, Richard Börner, Guillaume Mata, and Nathan W. Luedtke

*J. Am. Chem. Soc.*, **Just Accepted Manuscript** • DOI: 10.1021/jacs.0c05180 • Publication Date (Web): 11 Aug 2020

Downloaded from [pubs.acs.org](https://pubs.acs.org) on August 11, 2020

**Just Accepted**

“Just Accepted” manuscripts have been peer-reviewed and accepted for publication. They are posted online prior to technical editing, formatting for publication and author proofing. The American Chemical Society provides “Just Accepted” as a service to the research community to expedite the dissemination of scientific material as soon as possible after acceptance. “Just Accepted” manuscripts appear in full in PDF format accompanied by an HTML abstract. “Just Accepted” manuscripts have been fully peer reviewed, but should not be considered the official version of record. They are citable by the Digital Object Identifier (DOI®). “Just Accepted” is an optional service offered to authors. Therefore, the “Just Accepted” Web site may not include all articles that will be published in the journal. After a manuscript is technically edited and formatted, it will be removed from the “Just Accepted” Web site and published as an ASAP article. Note that technical editing may introduce minor changes to the manuscript text and/or graphics which could affect content, and all legal disclaimers and ethical guidelines that apply to the journal pertain. ACS cannot be held responsible for errors or consequences arising from the use of information contained in these “Just Accepted” manuscripts.

# A Highly Fluorescent Nucleobase Molecular Rotor

Ashkan Karimi<sup>a,b</sup>, Richard Börner<sup>a,c</sup>, Guillaume Mata<sup>a</sup>, Nathan W. Luedtke<sup>a,b,d\*</sup>

<sup>a</sup> Department of Chemistry, University of Zurich, CH-8057 Zurich, Switzerland

<sup>b</sup> Department of Chemistry, McGill University, H3A-0B8 Montreal, Canada

<sup>c</sup> Laserinstitut Hochschule Mittweida, University of Applied Sciences, 09648 Mittweida, Germany

<sup>d</sup> Department of Pharmacology and Therapeutics, McGill University, H3A-1A3 Montreal, Canada

## Supporting Information Placeholder

**ABSTRACT:** Fluorescent base analogs (FBAs) are powerful probes of nucleic acids' structures and dynamics. However, previously reported FBAs exhibit relatively low brightness and therefore limited sensitivity of detection. Here we report the hitherto brightest FBA that has ideal molecular rotor properties for detecting local dynamic motions associated with base pair mismatches. The new *trans*-stilbene annulated uracil derivative "tsT" exhibits bright fluorescence emissions in various solvents ( $\epsilon \times \Phi = 3,400 - 29,700 \text{ cm}^{-1} \text{ M}^{-1}$ ) and is highly sensitive to mechanical motions in duplex DNA ( $\epsilon \times \Phi = 150 - 4,250 \text{ cm}^{-1} \text{ M}^{-1}$ ). tsT is thereby a "smart" thymidine analog, exhibiting a 28-fold brighter fluorescence intensity when base paired with A as compared to T or C. Time-correlated single photon counting revealed that the fluorescence lifetime of tsT ( $\tau = 4 - 11 \text{ ns}$ ) was shorter than its anisotropy decay in well-matched duplex DNA ( $\theta = 20 \text{ ns}$ ), yet longer than the dynamic motions of base pair mismatches (0.1 - 10 ns). These properties enable unprecedented sensitivity in detecting local dynamics of nucleic acids.

Fluorescent nucleobase analogs (FBAs) provide powerful tools for probing nucleic acids' structures, dynamics and binding interactions.<sup>1,2</sup> Compared to conjugated fluorophores and intercalating dyes, FBAs have the advantage of highly precise positioning within RNA and DNA structures. However, fluorescence quenching of FBAs by neighboring residues via photo-induced electron transfer (PET) can dramatically limit their brightness.<sup>3-6</sup> For example, small electron-poor systems such as 2-aminopurine (2AP) are reductively quenched by purines,<sup>7</sup> and electron-rich systems such as <sup>MDA</sup> are oxidatively quenched by pyrimidines.<sup>8</sup> The brightest, previously reported fluorescent nucleobase analogs, such as tC<sup>o</sup> ( $\epsilon \times \Phi \approx 2,000 \text{ cm}^{-1} \text{ M}^{-1}$ ),<sup>9,10</sup> avoid PET quenching by having HOMO-LUMO energy levels that are intermediate between the HOMO of guanine and the LUMO of thymidine (Figure 1 and Figure S1). However, the fluorescence intensity of tC<sup>o</sup> and related analogs exhibit little-to-no environmental sensitivity and therefore have limited utility as reporters of base pair mismatches.<sup>11,12</sup> Given the growing clinical interest in point-of-care detection of single nucleotide polymorphisms (SNPs),<sup>13</sup> there have been numerous efforts towards the development of SNP sensors based on FBA-mismatch detection.<sup>8,14-27</sup> However, these

attempts have thus far resulted in either bright FBAs with low sensitivity towards SNPs,<sup>15-19</sup> or highly sensitive FBAs with low brightness.<sup>8,20,21</sup> Here we present the brightest and most sensitive FBA-mismatch reporter to date. The *trans*-stilbene-containing thymidine analog "tsT" acts as an ideal molecular rotor for SNP detection,<sup>22-27</sup> with a fluorescent lifetime ( $\tau = 4 - 11 \text{ ns}$ ) that is slightly longer as compared to timescale of local dynamic motions of base pair mismatches (0.1 - 10 ns).<sup>28-30</sup> This provides unprecedented sensitivity and specificity for detecting a single adenine residue in the opposing strand, with a ~20-fold brighter fluorescence intensity for matched "A" ( $\epsilon \times \Phi = 3,000 - 4,250 \text{ cm}^{-1} \text{ M}^{-1}$ ) versus mismatched "C, T, and G" bases ( $\epsilon \times \Phi = 150 - 520 \text{ cm}^{-1} \text{ M}^{-1}$ ).

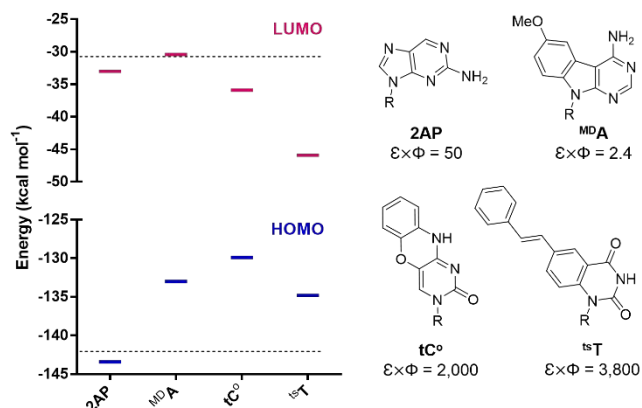
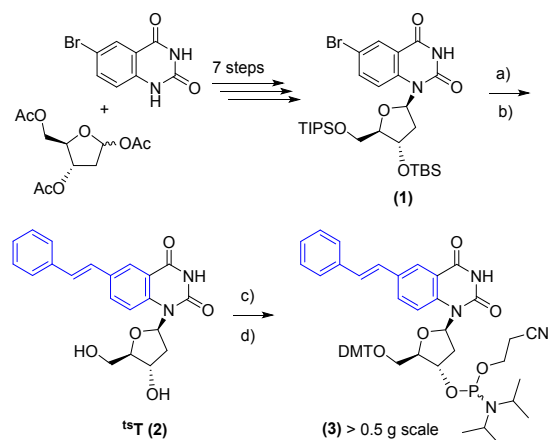


**Figure 1.** Average brightness of selected FBAs in well-matched duplex DNA ( $\text{cm}^{-1} \text{ M}^{-1}$ ) and their calculated HOMO-LUMO energy levels ( $\text{kcal mol}^{-1}$ ). DFT calculations (where R = Me) were performed using B3LYP/6-31+G(d) in water (see Table S1 and Figure S1 for details). The dashed lines represent the LUMO level of the most easily reduced nucleobase (T), and the HOMO level of the most easily oxidized base (G).<sup>31</sup>

Design of the new fluorescent thymidine analog "tsT" was inspired by the excellent base pairing specificities of 6-substituted quinazolines,<sup>19,32-34</sup> together with the desirable photophysical properties of *trans*-stilbene that include viscosity-sensitive emissions.<sup>35</sup> Density Functional Theory (DFT) calculations predicted that a ring-fused, uracil-*trans*-stilbene derivative "tsT" should not undergo fluorescence

quenching via PET (Figure 1). We therefore commenced synthesis of <sup>ts</sup>T by preparing 6-bromo-quinazoline-2,4-(3H)-dione nucleoside **1** as a single diastereoisomer on a multi-gram scale in a 46% overall yield (7 steps) according to our previously established protocol.<sup>36</sup> Suzuki-Miyaura coupling, followed by silyl deprotection furnished <sup>ts</sup>T nucleoside **2** in a 92% isolated yield over 2 steps (Scheme 1 and Scheme S1).

### Scheme 1. Synthesis of <sup>ts</sup>T nucleoside (**2**) and <sup>ts</sup>T phosphoramidite (**3**)<sup>a,b</sup>.



<sup>a</sup> Reagents and conditions: (a) *trans*-2-phenylvinyl boronic acid pinacol ester (2.1 equiv.), Cs<sub>2</sub>CO<sub>3</sub> (3.2 equiv.), Pd(dppf)Cl<sub>2</sub>, 1,4-dioxane, Ar, 100 °C, 24 h, (98%). (b) TBAF (4.9 equiv.), THF, 25 °C, 22 h, (94%). (c) DMTCl (1.4 equiv.), pyridine, Ar, 25 °C, 165 min, (68%). (d) 2-cyanoethyl N, N-diisopropyl chlorophosphoramidite (4.0 equiv.), DIPEA (5.0 equiv.), CH<sub>2</sub>Cl<sub>2</sub>, Ar, 0 to 25 °C, 150 min, (90%). TIPS = triisopropylsilyl, TBS = *tert*-butyldimethylsilyl, dppf = 1,1'-Bis(diphenylphosphino)ferrocene, TBAF = tetra-*n*-butylammoniumfluoride, THF = tetrahydrofuran, DMTCl = 4,4'-dimethoxytriphenylmethyl chloride, DIPEA = *N,N*-diisopropylethylamine. <sup>b</sup> See the SI for synthetic details and

As compared to *trans*-stilbene itself ( $\Phi = 0.02 - 0.04$ ), the <sup>ts</sup>T nucleoside **2** exhibits a similar extinction coefficient ( $\epsilon_{310\text{nm}} = 36,500 \pm 5,600 \text{ cm}^{-1} \text{ M}^{-1}$ ), yet much larger quantum yield ( $\Phi = 0.11 - 0.75$ ) in various solvents (Table S2). Decreasing quantum yields and increasing Stokes' shifts of nucleoside **2** were observed with increasing solvent polarity (Figure S2). These results are consistent with formation of a twisted intramolecular charge transfer (TICT) excited state leading to non-radiative decay.<sup>37,38</sup> To further evaluate the potential of <sup>ts</sup>T as a fluorescent molecular rotor, the absorption and fluorescence emission of nucleoside **2** was measured in various mixtures of methanol and glycerol. These solvents have very similar polarities yet drastically different viscosities. The quantum yield of

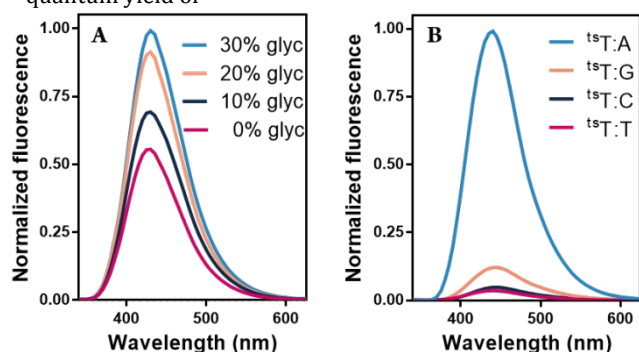


**Figure 2.** (A) Fluorescence of <sup>ts</sup>T nucleoside **2** in mixtures of methanol and glycerol; and (B) Fluorescence of <sup>ts</sup>T functionalized duplex DNA (ODN1) containing matched or mismatched base pairs in PBS buffer (pH = 7.4). All emission spectra were collected using an excitation wavelength of 310

nm. <sup>ts</sup>T increased with increasing viscosity (Figure 2A and Figure S3), consistent with rotation-induced fluorescent quenching. Encouraged by these results, we synthesized <sup>ts</sup>T phosphoramidite **3** for its incorporation into DNA. Nucleoside **2** was treated with DMTCl and chlorophosphoramidite to obtain >500 mg of pure <sup>ts</sup>T phosphoramidite **3**. The entire 11-step sequence required only 7 chromatographic separations and provided **3** in a 26% overall isolated yield.

Using standard, solid-phase supported synthesis,<sup>39</sup> <sup>ts</sup>T was incorporated into three different oligonucleotide DNAs (ODN1 – ODN3). Following their purification and annealing to complementary strands, canonical B-form secondary structures were observed using circular dichroism (Figure S6). The maximum absorbance of <sup>ts</sup>T remains very strong in DNA ( $\epsilon_{310\text{nm}} = 30,600 \pm 700 \text{ cm}^{-1} \text{ M}^{-1}$ ) and sufficiently red shifted to have no overlap with the natural bases (Fig S7A). The brightness of the three duplexes containing a <sup>ts</sup>T:A base pair ( $\epsilon \times \Phi = 3,000 - 4,250 \text{ cm}^{-1} \text{ M}^{-1}$ ) were about the same as the free nucleoside **2** in PBS buffer ( $3,420 \text{ cm}^{-1} \text{ M}^{-1}$ ), consistent with a lack of <sup>ts</sup>T fluorescence quenching by neighboring residues via PET. Thermal denaturation experiments revealed that <sup>ts</sup>T exhibits similar base pairing specificity as thymidine,<sup>40</sup> with the temperature of ODN1 duplex melting ( $T_m$ ) being <sup>ts</sup>T:C/T < <sup>ts</sup>T:G < <sup>ts</sup>T:A (Table 1 and Figure S8). The brightness of <sup>ts</sup>T was much more sensitive to this same trend, with  $\epsilon \times \Phi$  values ranging from 150 – 4,250  $\text{cm}^{-1} \text{ M}^{-1}$  for <sup>ts</sup>T:C/T < <sup>ts</sup>T:G << <sup>ts</sup>T:A (Table 1, Figure 2B and Figure S7B). Similar trends were also observed for the relative broadness of thymidine imino proton resonances in <sup>1</sup>H NMR spectra of T:G and T:T base pairs in duplex DNA.<sup>41</sup> Together these results suggested that fluorescence quenching of <sup>ts</sup>T is related to increased molecular motions of mismatched <sup>ts</sup>T:C/T base pairs over both <sup>ts</sup>T:G (wobble) and <sup>ts</sup>T:A base pairs.

**Table 1: Fluorescence quantum yield ( $\Phi$ ), brightness ( $\epsilon \times \Phi$ ) and melting temperature ( $T_m$ ) of double-stranded or single-stranded (ss) DNA.<sup>a</sup>**

Oligonucleotide	$\Phi$	$\epsilon \times \Phi$ ( $\text{cm}^{-1} \text{ M}^{-1}$ )	$T_m$ (°C)
<sup>ts</sup> T:A	0.139	4,250	55.0 <sup>c</sup>
<sup>ts</sup> T:G	0.017	520	53.0
<b>ODN1<sup>b</sup></b>			
<sup>ts</sup> T:C	0.005	150	51.0
<sup>ts</sup> T:T	0.005	150	50.8
ss- <sup>ts</sup> T	0.028	860	-
<sup>ts</sup> T:A	0.098	3,000	60.2 <sup>d</sup>
<b>ODN2<sup>b</sup></b>			
<sup>ts</sup> T:T	0.012	370	56.1
ss- <sup>ts</sup> T	0.020	610	-
<sup>ts</sup> T:A	0.134	4,100	54.1 <sup>e</sup>
<b>ODN3<sup>b</sup></b>			
ss- <sup>ts</sup> T	0.026	800	-

<sup>a</sup> All measurements were performed at 25 °C in PBS buffer (pH = 7.4), with DNA concentrations = 2.0  $\mu\text{M}$ . <sup>b</sup> ODN1 sequence: 5'-GCCGTA<sup>ts</sup>TCGTATACAC-3'. ODN2 sequence: 5'-GCCGTA<sup>ts</sup>TGCGTATACAC-3'. ODN3 sequence: 5'-GCCGTA<sup>ts</sup>TATGTATACAC-3'. <sup>c</sup>  $T_m$  of the corresponding unmodified duplex = 49.7 °C. <sup>d</sup>  $T_m$  of the unmodified duplex DNA = 56.3 °C. <sup>e</sup>  $T_m$  of the unmodified duplex DNA = 49.3 °C.

To gain insight into the relationships between  ${}^{\text{ts}}\text{T}$  dynamic motions and brightness in DNA, time-correlated single photon counting (TCSPC) experiments were conducted using  $ds\text{-}{}^{\text{ts}}\text{T:A}$ .<sup>a</sup> All measurements were performed using 2.0  $\mu\text{M}$  of DNA in PBS buffer (pH = 7.4). All values reflect averages and standard deviations of three measurements.<sup>b</sup> See Table S5 for details. <sup>c</sup> Calculated from  $E\theta$  (Eq. S5). <sup>d</sup> Value reflects local dynamics, not  $R_{\text{H}}$ .

${}^{\text{ts}}\text{T:T}$  (4.5 ns), reflecting the same trends as their steady-state brightness. Upon heating each sample over a “pre-melting” temperature range of 25  $^{\circ}\text{C}$   $\rightarrow$  45  $^{\circ}\text{C}$  where no global melting of the duplexes was observed, the  $\tau$  values of  ${}^{\text{ts}}\text{T}$  decreased in a linear fashion for both  $ds\text{-}{}^{\text{ts}}\text{T:A}$  (-0.11 ns per  $^{\circ}\text{C}$ ) and  $ss\text{-}{}^{\text{ts}}\text{T}$  (-0.05 ns per  $^{\circ}\text{C}$ , Figure 3A). These results are consistent with increased “breathing” motions of nucleobases with increasing temperatures.<sup>42</sup> Surprisingly, the  $\tau$  values of  $ds\text{-}{}^{\text{ts}}\text{T:T}$  increased over this same temperature range (+0.03 ns per  $^{\circ}\text{C}$ ), suggesting increasing rigidity of the mismatch with increasing temperature. This result is consistent with the higher affinity and positive entropy change exhibited by T:T mismatches for Hg<sup>II</sup> binding over these temperatures.<sup>43,44</sup> At 55  $^{\circ}\text{C}$  the  $\tau$  values for all three samples neared convergence due to thermal melting of the duplexes (Figure 3A).

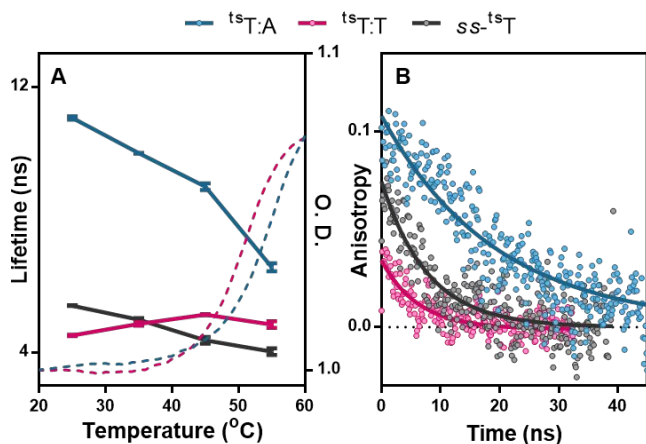


**Figure 3.** (A) Temperature-dependent fluorescence lifetime values (averaged values of three measurements with standard errors connected by solid lines) compared to global thermal melting according to absorbance changes (O.D., dashed lines) at 260 nm. (B) Time-resolved fluorescence anisotropy of  $ss\text{-}{}^{\text{ts}}\text{T}$ ,  $ds\text{-}{}^{\text{ts}}\text{T:T}$  and  $ds\text{-}{}^{\text{ts}}\text{T:A}$  (ODN1) at 25  $^{\circ}\text{C}$ . All measurements were conducted in PBS buffer (pH = 7.4).

**Table 2. Fluorescence lifetime ( $\tau$ ), anisotropy decay ( $\theta$ ), and hydrodynamic radius ( $R_{\text{H}}$ ) of ODN1 double-stranded or single-stranded (ss).<sup>a, b</sup>**

	T ( $^{\circ}\text{C}$ )	$\tau$ (ns)	$\theta$ (ns)	$R_{\text{H}}$ (nm) <sup>c</sup>
${}^{\text{ts}}\text{T:A}$	25	$11.1 \pm 0.1$	$20 \pm 4.2$	$2.70 \pm 0.18$
	35	$10.0 \pm 0.1$	$19 \pm 3.8$	$2.68 \pm 0.18$
	55	$6.6 \pm 0.1$	$8.5 \pm 2.8$	$2.09 \pm 0.22$
${}^{\text{ts}}\text{T:T}$	25	$4.5 \pm 0.1$	$5.3 \pm 1.6$	$1.74 \pm 0.17^{\text{d}}$

$ss\text{-}{}^{\text{ts}}\text{T}$	25	$5.4 \pm 0.1$	$7.9 \pm 1.7$	$1.98 \pm 0.14$
------------------------------------	----	---------------	---------------	-----------------

To evaluate local and global dynamic motions, TCSPC experiments were used to measure time-resolved fluorescence anisotropy decay ( $\theta$ , Figure 3B, Eq. S4). At 25  $^{\circ}\text{C}$ , the  $\theta$  values of  ${}^{\text{ts}}\text{T}$  in DNA followed the same trends as steady-state quantum yields and fluorescence lifetime measurements, where  $ds\text{-}{}^{\text{ts}}\text{T:A}$  ( $\theta = 20$  ns)  $\gg$   $ss\text{-}{}^{\text{ts}}\text{T}$  ( $\theta = 7.9$  ns)  $>$   $ds\text{-}{}^{\text{ts}}\text{T:T}$  ( $\theta = 5.3$  ns). The  $\theta$  values of  $ds\text{-}{}^{\text{ts}}\text{T:A}$  at 25  $^{\circ}\text{C}$  and 35  $^{\circ}\text{C}$  were essentially identical ( $\theta = 19 - 20$  ns, Table 2 and Figure S10), suggesting that the  $\theta$  values are reflecting global motions of the duplex at these temperatures. We therefore used the  $\theta$  value at 25  $^{\circ}\text{C}$  to calculate the hydrodynamic radius of the duplex ( $R_{\text{H}}$ , Eq. S5), giving  $R_{\text{H}} = 2.70 \pm 0.18$  nm (Table 2). This value is in full agreement with duplex DNA  $R_{\text{H}}$  values previously measured using fluorescence anisotropy, sedimentation velocity and Monte Carlo simulations.<sup>9,45,46</sup> At 55  $^{\circ}\text{C}$  the  $\theta$  of  $ds\text{-}{}^{\text{ts}}\text{T:A}$  (8.5 ns) approached that of  $ss\text{-}{}^{\text{ts}}\text{T}$  at 25  $^{\circ}\text{C}$  (7.9 ns). These values are consistent with the conversion of a “rod-like” duplex ( $R_{\text{H}} = 2.70$  nm) into a “worm-like” chain of ssDNA ( $R_{\text{H}} = 2.09$  nm, Table 2).<sup>47,48</sup> The close agreements between our results obtained using  ${}^{\text{ts}}\text{T}$  with the global physical properties of ssDNA,<sup>49,50</sup> suggest that ssDNA contains partially-ordered nucleobases with correlation times dominated by concerted, global motions of the entire molecule. In contrast, the  $\theta$  for mismatched, duplex  $ds\text{-}{}^{\text{ts}}\text{T:T}$  (5.3 ns) primarily reflects rapid, local dynamics, since this value is much lower than that of  $ds\text{-}{}^{\text{ts}}\text{T:A}$  (20 ns), and it is even lower than  $ss\text{-}{}^{\text{ts}}\text{T}$  at 25  $^{\circ}\text{C}$  (7.9 ns). These results are consistent with previous NMR measurements and molecular dynamics simulations suggesting the presence of rapid, local motions of base pair mismatches in otherwise canonical duplexes.<sup>28</sup> To our knowledge this is the first time that an FBA has been used to determine the hydrodynamic radii of single-stranded DNA, and our results suggest that the dynamic motions of a base pair mismatch in duplex DNA are even greater than those present in single-stranded DNA.

In summary,  ${}^{\text{ts}}\text{T}$  is the brightest and most environment sensitive FBA reported to date ( $\epsilon \times \Phi = 150 - 29,700$   $\text{cm}^{-1} \text{M}^{-1}$ ). The fluorescence lifetime of  ${}^{\text{ts}}\text{T}$  ( $\tau = 4 - 11$  ns) is longer than the time scale of local dynamic motions of base pair mismatches (0.1 - 10 ns),<sup>28-30</sup> yet faster than the global anisotropy decay of  ${}^{\text{ts}}\text{T}$  in duplex DNA ( $\theta = 20$  ns). These properties together enable unprecedented sensitivity and specificity in the detection of an adenine residue in the complement strand. In addition to highly sensitive base pair match/mismatch discrimination,  ${}^{\text{ts}}\text{T}$  has provided insights into the fundamental dynamic behavior of duplex and single-stranded DNA using TCSPC experiments. The exceptional brightness and sensitivity of  ${}^{\text{ts}}\text{T}$  may enable other types of demanding applications, such as tracking of single-molecule dynamics.<sup>51</sup>

## ASSOCIATED CONTENT

### Supporting Information

The Supporting Information is available free of charge on the ACS Publications website. Description of materials and methods, computational details, synthetic procedures, compounds characterization and NMR spectra, circular

dichroism (CD), thermal denaturation (T<sub>m</sub>) and fluorescence spectra, Scheme S1, Figures S1-S10 and Tables S1-S5.

## AUTHOR INFORMATION

### Corresponding Author

Email: nathan.luedtke@mcgill.ca

### Notes

The authors declare no competing financial interests.

### ACKNOWLEDGMENT

We thank Prof. R. K. O. Sigel for his support of R.B. We thank the University of Zurich, McGill University, University of Applied Sciences Mittweida, the Swiss National Science Foundation (grant No. 165949 to N.W.L), the National Research Council of Canada (grant No. 05048 to N.W.L), and the McGill Centre for Structural Biology (studentship to A.K.) for funding.

## REFERENCES

- Xu, W.; Chan, K. M.; Kool, E. T., Fluorescent Nucleobases as Tools for Studying DNA and RNA. *Nat Chem* **2017**, *9* (11), 1043–1055.
- Michel, B. Y.; Dziuba, D.; Benhida, R.; Demchenko, A. P.; Burger, A., Probing of Nucleic Acid Structures, Dynamics, and Interactions With Environment-Sensitive Fluorescent Labels. *Front Chem* **2020**, *8*, 112.
- Johnson, A.; Karimi, A.; Luedtke, N. W., Enzymatic Incorporation of a Coumarin–Guanine Base Pair. *Angew Chem Int Ed* **2019**, *58* (47), 16839–16843.
- Hawkins, M. E.; Balis, F. M., Use of Pteridine Nucleoside Analogs as Hybridization Probes. *Nucleic Acids Res* **2004**, *32* (7), e62.
- Wojciechowski, F.; Hudson, R. H. E., Fluorescence and Hybridization Properties of Peptide Nucleic Acid Containing a Substituted Phenylpyrrolocytosine Designed to Engage Guanine with an Additional H-Bond. *J Am Chem Soc* **2008**, *130* (38), 12574–12575.
- Hudson, R. H. E.; Ghorbani-Choghamarani, A., Selective Fluorometric Detection of Guanosine-Containing Sequences by 6-Phenylpyrrolocytidine in DNA. *Synlett* **2007**, *2007* (06), 870–873.
- Narayanan, M.; Kodali, G.; Xing, Y.; Stanley, R. J., Photoinduced Electron Transfer Occurs between 2-Aminopurine and the DNA Nucleic Acid Monophosphates: Results from Cyclic Voltammetry and Fluorescence Quenching. *J Phys Chem B* **2010**, *114* (32), 10573–10580.
- Okamoto, A.; Tanaka, K.; Fukuta, T.; Saito, I., Design of Base-Discriminating Fluorescent Nucleoside and Its Application to T/C SNP Typing. *J Am Chem Soc* **2003**, *125* (31), 9296–9297.
- Sandin, P.; Börjesson, K.; Li, H.; Mårtensson, J.; Brown, T.; Wilhelmsson, L. M.; Albinsson, B., Characterization and Use of an Unprecedentedly Bright and Structurally Non-Perturbing Fluorescent DNA Base Analogue. *Nucleic Acids Res* **2008**, *36* (1), 157–167.
- Bood, M.; Fuchtbauer, A. F.; Wranne, M. S.; Ro, J. J.; Sarangamath, S.; El-Sagheer, A. H.; Rupert, D. L. M.; Fisher, R. S.; Magennis, S. W.; Jones, A. C.; Hook, F.; Brown, T.; Kim, B. H.; Dahlen, A.; Wilhelmsson, L. M.; Groth, M., Pentacyclic Adenine: a Versatile and Exceptionally Bright Fluorescent DNA Base Analogue. *Chem Sci* **2018**, *9* (14), 3494–3502.
- Jean, J. M.; Hall, K. B., 2-Aminopurine Fluorescence Quenching and Lifetimes: Role of Base Stacking. *Proc Natl Acad Sci USA* **2001**, *98* (1), 37.
- Dueymes, C.; Décout, J. L.; Peltié, P.; Fontecave, M., Fluorescent Deazaflavin–Oligonucleotide Probes for Selective Detection of DNA. *Angew Chem Int Ed* **2002**, *41* (3), 486–489.
- Xu, H.; Xia, A.; Wang, D.; Zhang, Y.; Deng, S.; Lu, W.; Luo, J.; Zhong, Q.; Zhang, F.; Zhou, L.; Zhang, W.; Wang, Y.; Yang, C.; Chang, K.; Fu, W.; Cui, J.; Gan, M.; Luo, D.; Chen, M., An ultraportable and versatile point-of-care DNA testing platform. *Science Advances* **2020**, *6* (17), eaaz7445.
- Hwang, G. T., Single-Labeled Oligonucleotides Showing Fluorescence Changes Upon Hybridization with Target Nucleic Acids. *Molecules* **2018**, *23* (1), 124.
- Sandin, P.; Wilhelmsson, L. M.; Lincoln, P.; Powers, V. E. C.; Brown, T.; Albinsson, B., Fluorescent Properties of DNA Base Analogue tC upon Incorporation Into DNA – Negligible Influence of Neighbouring Bases on Fluorescence Quantum Yield. *Nucleic Acids Res* **2005**, *33* (16), 5019–5025.
- Burns, D. D.; Teppang, K. L.; Lee, R. W.; Lokensgard, M. E.; Purse, B. W., Fluorescence Turn-On Sensing of DNA Duplex Formation by a Tricyclic Cytidine Analogue. *J Am Chem Soc* **2017**, *139* (4), 1372–1375.
- Teppang, K. L.; Lee, R. W.; Burns, D. D.; Turner, M. B.; Lokensgard, M. E.; Cooksy, A. L.; Purse, B. W., Electronic Modifications of Fluorescent Cytidine Analogues Control Photophysics and Fluorescent Responses to Base Stacking and Pairing. *Chem Eur J* **2019**, *25* (5), 1249–1259.
- Gardarsson, H.; Kale, A. S.; Sigurdsson, S. T., Structure–Function Relationships of Phenoxazine Nucleosides for Identification of Mismatches in Duplex DNA by Fluorescence Spectroscopy. *Chembiochem* **2011**, *12* (4), 567–575.
- Mata, G.; Schmidt, O. P.; Luedtke, N. W., A Fluorescent Surrogate of Thymidine in Duplex DNA. *Chem Commun* **2016**, *52* (25), 4718–4721.
- Okamoto, A.; Tainaka, K.; Saito, I., Clear Distinction of Purine Bases on the Complementary Strand by a Fluorescence Change of a Novel Fluorescent Nucleoside. *J Am Chem Soc* **2003**, *125* (17), 4972–4973.
- Miyata, K.; Tamamushi, R.; Ohkubo, A.; Taguchi, H.; Seio, K.; Santa, T.; Sekine, M., Synthesis and Properties of a New Fluorescent Bicyclic 4-N-Carbamoyldeoxycytidine Derivative. *Org Lett* **2006**, *8* (8), 1545–1548.
- Greco, N. J.; Sinkeldam, R. W.; Tor, Y., An Emissive C Analog Distinguishes between G, 8-oxoG, and T. *Org Lett* **2009**, *11* (5), 1115–1118.
- Saito, Y.; Motegi, K.; Bag, S. S.; Saito, I., Anthracene Based Base-Discriminating Fluorescent Oligonucleotide Probes for SNPs Typing: Synthesis and Photophysical Properties. *Biorg Med Chem* **2008**, *16* (1), 107–113.
- Suzuki, A.; Saito, M.; Katoh, R.; Saito, Y., Synthesis of 8-Aza-3,7-dideaza-2'-deoxyadenosines Possessing a New Adenosine Skeleton as an Environmentally Sensitive Fluorescent Nucleoside for Monitoring the DNA Minor Groove. *Org Biomol Chem* **2015**, *13* (27), 7459–7468.
- Güixens-Gallardo, P.; Humpolickova, J.; Miclea, S. P.; Pohl, R.; Kraus, T.; Jurkiewicz, P.; Hof, M.; Hocek, M., Thiophene-Linked Tetramethylbodipy-Labeled Nucleotide for Viscosity-Sensitive Oligonucleotide Probes of Hybridization and Protein–DNA Interactions. *Org Biomol Chem* **2020**, *18* (5), 912–919.
- Liu, L.; Shao, Y.; Peng, J.; Liu, H.; Zhang, L., Selective Recognition of ds-DNA Cavities by a Molecular Rotor: Switched Fluorescence of Thioflavin T. *Mol Biosyst* **2013**, *9* (10), 2512–2519.
- Ryu, J. H.; Seo, Y. J.; Hwang, G. T.; Lee, J. Y.; Kim, B. H., Triad Base Pairs Containing Fluorene Unit for Quencher-Free SNP Typing. *Tetrahedron* **2007**, *63* (17), 3538–3547.
- Rossetti, G.; Dans, P. D.; Gomez-Pinto, I.; Ivani, I.; Gonzalez, C.;

- Orozco, M., The Structural Impact of DNA Mismatches. *Nucleic Acids Res* **2015**, *43* (8), 4309—4321.
29. Shweta, H.; Singh, M. K.; Yadav, K.; Verma, S. D.; Pal, N.; Sen, S., Effect of T·T Mismatch on DNA Dynamics Probed by Minor Groove Binders: Comparison of Dynamic Stokes Shifts of Hoechst and DAPI. *J Phys Chem B* **2017**, *121* (48), 10735—10748.
30. Isaacs, R. J.; Rayens, W. S.; Spielmann, H. P., Structural Differences in the NOE-Derived Structure of G–T Mismatched DNA Relative to Normal DNA are Correlated with Differences in 13C Relaxation-Based Internal Dynamics. *J Mol Biol* **2002**, *319* (1), 191—207.
31. Seidel, C. A. M.; Schulz, A.; Sauer, M. H. M., Nucleobase-Specific Quenching of Fluorescent Dyes. 1. Nucleobase One-Electron Redox Potentials and Their Correlation with Static and Dynamic Quenching Efficiencies. *J Phys Chem* **1996**, *100* (13), 5541—5553.
32. Krueger, A. T.; Lu, H.; Lee, A. H. F.; Kool, E. T., Synthesis and Properties of Size-Expanded DNAs: Toward Designed, Functional Genetic Systems. *Acc Chem Res* **2007**, *40* (2), 141—150.
33. Xie, Y.; Maxson, T.; Tor, Y., Fluorescent Nucleoside Analogue Displays Enhanced Emission upon Pairing with Guanine. *Org Biomol Chem* **2010**, *8* (22), 5053—5055.
34. Hirashima, S.; Han, J. H.; Tsuno, H.; Tanigaki, Y.; Park, S.; Sugiyama, H., New Size-Expanded Fluorescent Thymine Analogue: Synthesis, Characterization, and Application. *Chem Eur J* **2019**, *25* (42), 9913—9919.
35. Wilhelm Hans, E.; Gebert, H.; Regenstein, W., Effect of Substituents on the Viscosity Dependence of Fluorescence and on the S1 - T1 Energy Gap of Donor-Acceptor Substituted Trans-Stilbenes. *Z Naturforsch, A: Phys Sci* **1997**, *52* (12), 837.
36. Mata, G.; Luedtke, N. W., Stereoselective N-Glycosylation of 2-Deoxythioribosides for Fluorescent Nucleoside Synthesis. *J Org Chem* **2012**, *77* (20), 9006—9017.
37. Waldeck, D. H., Photoisomerization Dynamics of Stilbenes. *Chem Rev* **1991**, *91* (3), 415—436.
38. Steffen, F. D.; Sigel, R. K. O.; Börner, R., An Atomistic View on Carbocyanine Photophysics in the Realm of RNA. *Phys Chem Chem Phys* **2016**, *18* (42), 29045—29055.
39. Abramova, T., Frontiers and Approaches to Chemical Synthesis of Oligodeoxyribonucleotides. *Molecules* **2013**, *18* (1), 1063—1075.
40. Aboul-ela, F.; Koh, D.; Tinoco, I., Jr.; Martin, F. H., Base-Base Mismatches. Thermodynamics of Double Helix Formation for dCA3XA3G + dCT3YT3G (X, Y = A,C,G,D). *Nucleic Acids Res* **1985**, *13* (13), 4811—4824.
41. Schmidt, O. P.; Jurt, S.; Johannsen, S.; Karimi, A.; Sigel, R. K. O.; Luedtke, N. W., Concerted Dynamics of Metallo-Base Pairs in an A/B-Form Helical Transition. *Nat Commun* **2019**, *10* (1), 4818.
42. Brunet, A.; Salomé, L.; Rousseau, P.; Destainville, N.; Manghi, M.; Tardin, C., How Does Temperature Impact the Conformation of Single DNA Molecules Below Melting Temperature? *Nucleic Acids Res* **2018**, *46* (4), 2074—2081.
43. Torigoe, H.; Ono, A.; Kozasa, T., HgII Ion Specifically Binds with T:T Mismatched Base Pair in Duplex DNA. *Chem Eur J* **2010**, *16* (44), 13218-13225.
44. Schmidt, O. P.; Benz, A. S.; Mata, G.; Luedtke, N. W., HgII Binds to C-T Mismatches with High affinity. *Nucleic Acids Res* **2018**, *46* (13), 6470—6479.
45. Bonifacio, G. F.; Brown, T.; Conn, G. L.; Lane, A. N., Comparison of the Electrophoretic and Hydrodynamic Properties of DNA and RNA Oligonucleotide Duplexes. *Biophys J* **1997**, *73* (3), 1532—1538.
46. Fernandes, M. X.; Ortega, A.; Lopez Martinez, M. C.; Garcia de la Torre, J., Calculation of Hydrodynamic Properties of Small Nucleic Acids from Their Atomic Structure. *Nucleic Acids Res* **2002**, *30* (8), 1782—1788.
47. Tinland, B.; Pluen, A.; Sturm, J.; Weill, G., Persistence Length of Single-Stranded DNA. *Macromolecules* **1997**, *30* (19), 5763—5765.
48. Uzawa, T.; Cheng, R. R.; Cash, K. J.; Makarov, D. E.; Plaxco, K. W., The Length and Viscosity Dependence of End-to-End Collision Rates in Single-Stranded DNA. *Biophys J* **2009**, *97* (1), 205—210.
49. Doose, S.; Barsch, H.; Sauer, M., Polymer properties of polythymine as revealed by translational diffusion. *Biophys J* **2007**, *93* (4), 1224—1234.
50. Sim, A. Y.; Lipfert, J.; Herschlag, D.; Doniach, S., Salt dependence of the radius of gyration and flexibility of single-stranded DNA in solution probed by small-angle x-ray scattering. *Phys Rev E Stat Nonlin Soft Matter Phys* **2012**, *86* (2 Pt 1), 021901.
51. Nobis, D.; Fisher, R. S.; Simmermacher, M.; Hopkins, P. A.; Tor, Y.; Jones, A. C.; Magennis, S. W., Single-Molecule Detection of a Fluorescent Nucleobase Analogue via Multiphoton Excitation. *J Phys Chem Lett* **2019**, *10* (17), 5008—5012.

## Table of Contents artwork

